Design of Tunable Optical Band Pass Filter based on in-Line PM-Mach Zehnder Interferometer

Baraa H. Mutar[1] and Tahreer S. Mansour[1,*]

Corresponding author: Tahreer@ilps.uobaghdad.edu.iq

1-   *Institute of Laser for Postgraduate Studied, University of Baghdad, Baghdad, Iraq.*

Abstract: In this paper, tunable optical band-pass filters based on Polarization Maintaining Fiber –Mach Zehnder Interferometer presented. Tunability of the band-pass filter implemented by applying different mechanical forces N on the micro-cavities splicing regions (MCSRs). The micro-cavity formed by using three variable-lengths of single-mode polarization-maintaining fiber with (8, 16, 24) cm lengths, splice between two segments of (SMF-28) with (26, 13) cm lengths, using the fusion splicing technique. Ellipsoidal shape micro-cavities experimentally achieved parallel to the propagation axis having dimensions between (12-24) μm of width and   (4-12) μm of length. A micro-cavity with width and length as high as 24 μm and 12 μm have higher sensitivity of 0.00115 μƐ when 0.098 N applied to the micro-cavity splicing region. And full width half maximum was obtained 251.584 pm when polarization-maintaining fiber length was 16 cm after applied 0.49N on the micro-cavity splicing region. The pulsed laser source used in this experiment has peak power 1.2297mW, 286 pm spatial FWHM, and centered at 1546.7 nm.

Keywords: Polarization Maintaining Fiber(PMF), Mach-zehnder interferometer(MZI), Micro-stain, FWHM, MCSRs.

1.Introduction

In optical systems, optical filters are intensively employed. A tunable optical band-pass filter based on micro-cavities is one attractive optically component due to its compact size and high sensitivity. An optical tunable band-pass filter is an essential component to achieve maximum signal-to-noise ratio after decreasing phase intensity noise and multi-able access interference. These optical fibers are uses in different applications like fiber sensing, spectroscopic analysis, optical fiber laser, and optically filtering [1-5]. Furthermore, the ability of sensing is increase by utilizing innovative fiber optic technologies of fiber gratings, fiber interferometers, micro-structured fibers, nano-wires,   fiber coupler ,etc.[6]. Interferometers are one of the important types

because of their high sensitivities and relaxed requirements on the optical source power stability. Interferometer work by splitting the coherent light beam into two or more paths, then recombining them to interfere with the difference in path length between them produces the interference [7-9]. The path length difference was measured using an interferometer as a function of strain. Many different interferometers were designed as a result of these multiple. Because of its compactness and robustness, the in-line fiber interferometer attracted more attention, and it was built with a variety of optical fibers, including traditional fibers: single mode, multimode fibers, with fiber bragg grating, or photonic crystal fiber [10-12]. In this experiment, polarization-maintaining fiber was used, which is a special type of fiber

that can retain linear polarized states of light propagation over a long distance on a single-mode waveguide. SM-PM fibers also have a wide range of applications in the telecommunications and sensor fields[13,14]. Recently Panda-PMF have dominated on most of the applications because they're flexible and compatible with regular telecommunication optical fiber optic sensors offer numerous advantages over electric transducers due to their small size, high sensitivity, and the possibility of distributed measurements. optical fiber offers different alternatives for the fabrication of modal interferometers, where different types of fibers exist and can be used to build interferometers [15,16]. The main types of modal interferometer filters are Mach-Zehnder, Michelson, Sagnac, and the Fabry-Perot interferometers[17]. Many interferometers nowadays were designed for remote sensing applications that are constructed using different types of fibers and arrangements.

In (2015), Fahad M. Abdulhussein, et al. used two schemes for simultaneous measurements sensors , the first one is with dual FBGs peaks. Every FBG acts as sensing head. The first peak was used for temperature sensing and the obtained sensitivity is 10 pm/°C and the second peak was used for temperature and pressure measurements with sensitivities 9.2 pm/°C and 67 pm/ bar for temperature and pressure respectively [18, 19]. In (2018) Sura Hussein, et al. implemented a pulse compressor using a tunable hybrid Mach-Zehnder interferometer made from 7 and 19 cell hollow-core photonic crystal fibers after applying mechanical forces along the fiber cross-sectional [20]. Nowadays, new type of interferometer was designed using all fiber micro cavity Mach-Zender interferometer and the cavity region can be either air [21] or fiber spliced regions [22]. In this paper, the effects of applying mechanical forces in (N) on the micro splicing regions of the PM-MZI investigated to obtained tunable optical band pass filter.

2. Experimental setups

The single PM-MZI consists of one PM-MZI that means two micro cavity splicing regions (MCSRs), one cavity length (Lc), the mechanical force in (g) was varied from (0.049,0.098, 0.196, 0.49, and 0.98)(N) applied on the interferometer micro–cavities splicing regions. Figure (1) shows the schematic diagram

for the experimental setup for the tunable singe PM-Mach Zehnder interferometer.
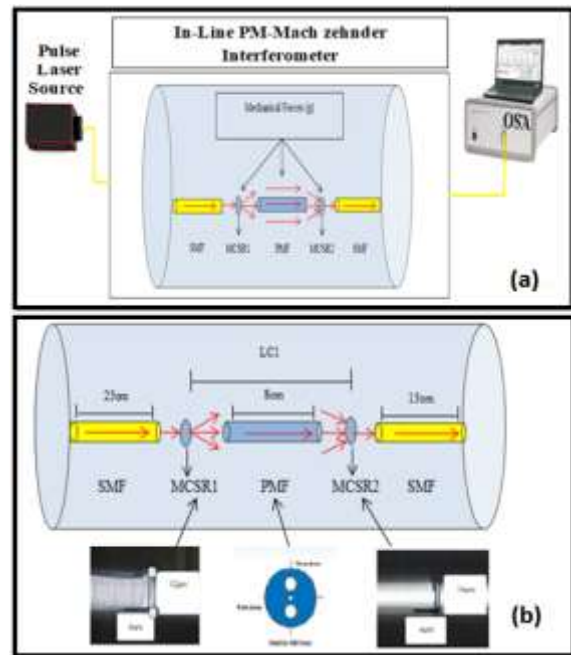
Figure (1): schematic diagram of (a) single PM-MZI (b) PM-MZI splicing regions.

In this experiment, an optical pulse laser source launched to PM-Mach Zehnder Interferometer. PM-MZI was building by using PMF with three different lengths (8,16,24) cm sandwiching between two standard single-mode optical fibers (SMF-28e) with length (23 and 13) cm. The cladding modes are excited by the first up-taper and then enter the PMF section as the interferometer arm. Finally, both the cladding modes and the core mode are reconnecting to the second up-taper. Then it was visualized by using an optical spectrum analyzer (OSA202). Figure (2) shows the photograph of the system setups.
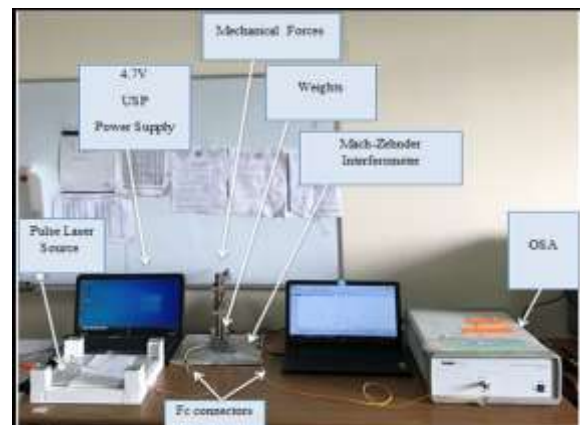
Figure (2): The experimental setup for In-line single PM-MZI.

The mechanical force was used to tune the phase of the optical signal on one arm of the PM-MZI. The applied forces imposed stress on the fiber caused elongation in the length of the fiber. The amount of the fiber elongation can be calculated using equations (1)(2),(3) [22-26]:

$$\text{the strain} = \frac{\Delta L}{L} = \frac{stress}{young\ modulus} \quad (1)$$

$$\text{stress} = \frac{Force\ (N)}{Area\ (m^2)} \quad (2)$$

$$F = m \times G \quad (3)$$

Where: L, is the original length, ΔL is the change in length, F, is the force applied in (N), A, is the cross sectional area in (m^2), m, is the value of the standard weight mass used to induce mechanical force and G, is the gravitational acceleration.

Young's modulus is the modulus of elasticity ranges from 66 Gpa to 74 Gpa for the SiO2 i.e 70 Gpa.

The mechanical forces in this work were done by applying different forces (0.049, 0.098, 0.196, 0.49, and 0.98) (N) on the micro cavity splicing regions of Pm-MZI. The young modulus for the optical fiber (i.e., SiO2).

3. Results

The results divide into two parts, the first part relationship between the force applied on the micro-cavities splicing regions with the strain and the second part for the mechanical force applied on the PM-MZI's micro splicing regions.

3.1 Result for strain effect

Due to the high sensitivity of this interferometer, the strain measurement is calculated to explain the ability of this interfrometer for withstanding of various values for harsh conditions. The values of strain that have been calculated will increase after increasing external force that applied on the micro cavities splicing regions.

The obtained experimental results of strain measurement will be divided according to the change length of Polarization maintaining fibers that used in interferometers. The values of the mass in g was converted to the force in N, this conversion process has been evaluated according to equation (3). The increase in the force that applied on the micro-cavity leads to an increase in the strain as seen in the figure (3), the solid line indicates. To the effect of force on

the first micro cavities splicing regions, and the dotted line indicates effect of force on the second micro cavities splicing regions.
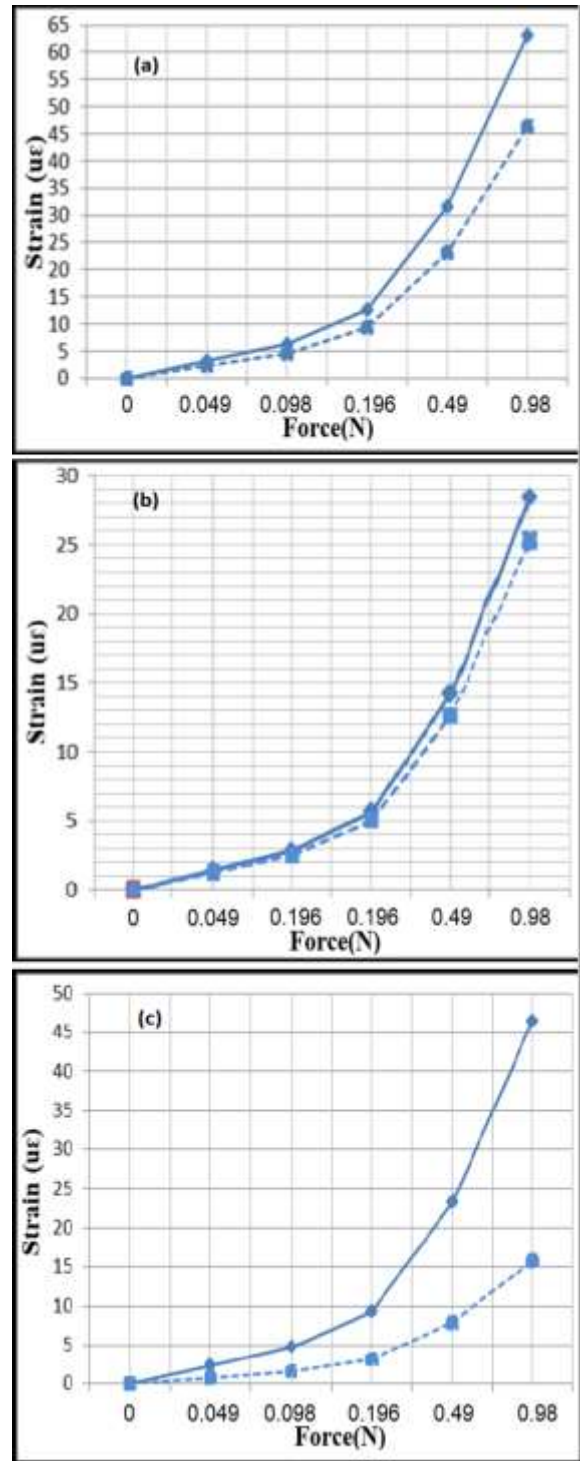
Figure(3): The relation between Mechanical force and strain ($\mu\varepsilon$) with three different length of PMF (a)8cm, (b)16cm and (c)24cm.

3.2 Results for force effect

The output spectrum of the PM-Mach Zehnder interferometer was visualized by using an

optical spectrum analyzer (OSA202), after applying different mechanical forces, on their micro cavities splicing regions, as shown in figure (4).
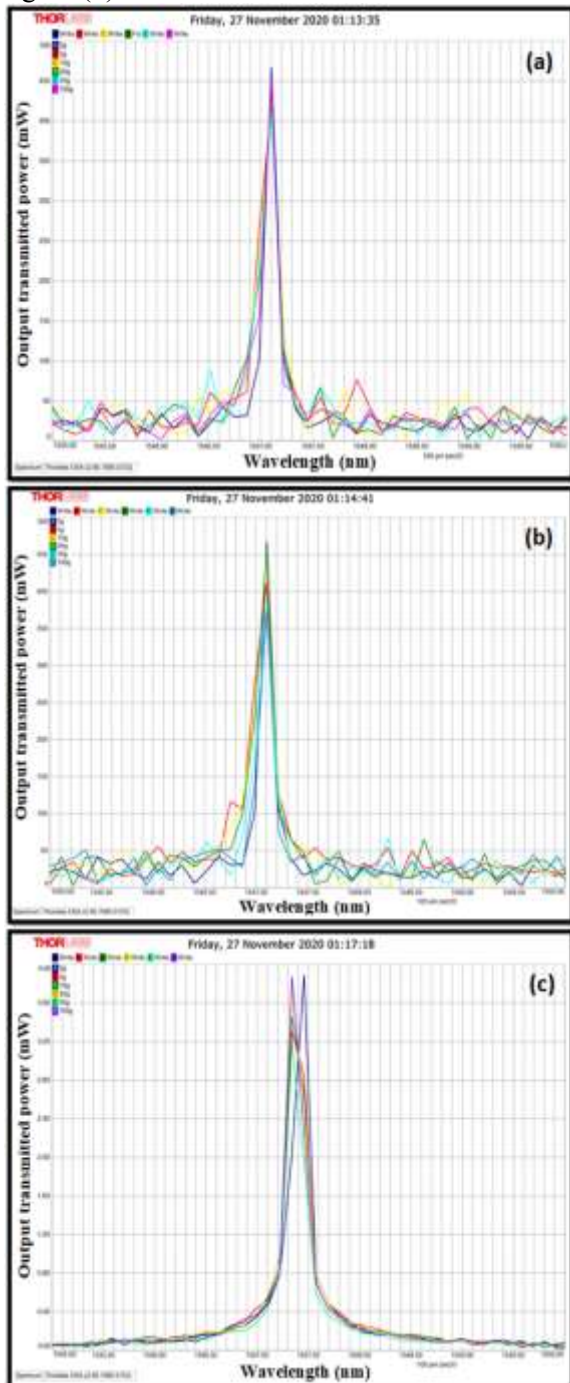
Figure(4): The spectrum of the output laser source after applying different weights on the micro cavities splicing regions with three different length of PMF ,(a) 8 cm, (b)16 cm and (c) 24 cm.

When the force was applied on PM-MZI cavity The elongation for micro cavity splicing region of PM-MZI will be reducing of the geometric parameters of PMF, this change of parameters caused decreased the group velocity

for all modes which propagated through the core and cladding for the fiber and the reducing in parameters of fiber will be changed on the parameters of pulse that propagated through the fiber. Figure (5) show the output spectra of PM-Mach Zehnder Interferometer due to the force effect, that was obtained by applying different values of force on the micro- cavity of PM-MZI with three different length. The increase in the force applied to the micro-cavity leads to an increase in the FWHM. The highest spectral width 251.58 (μm) has been gained when the PMF was 16 cm length and 0,049 force applied on micro cavity splicing regions.
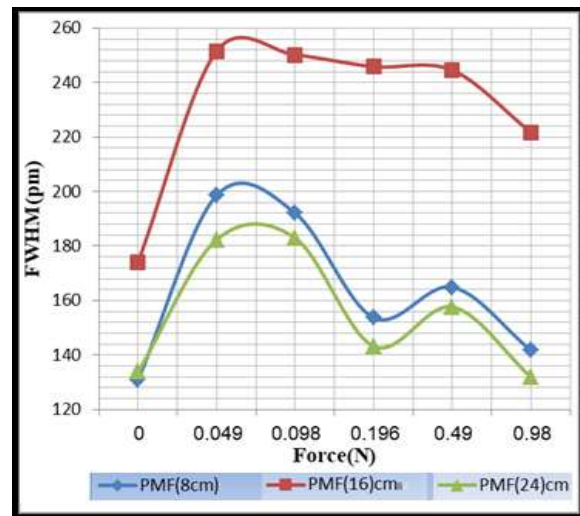
Figure(5): The Full Width Half Maximum variation of PM-MZI with (8,16,24cm) and different forces applied on micro cavities splicing regions.

The highest peak power value was recorded result in the case of 24cm PMF when no force was applied to it. Figure (6) show the peak power of the PM-Mach Zehnder interferometer after applying different values of force N on the micro-cavities splicing regions.
The wavelength shift of the PM-MZI spectrum is very clear due to the different values of forces applied on the micro-cavity splicing region as shown in figure (7).
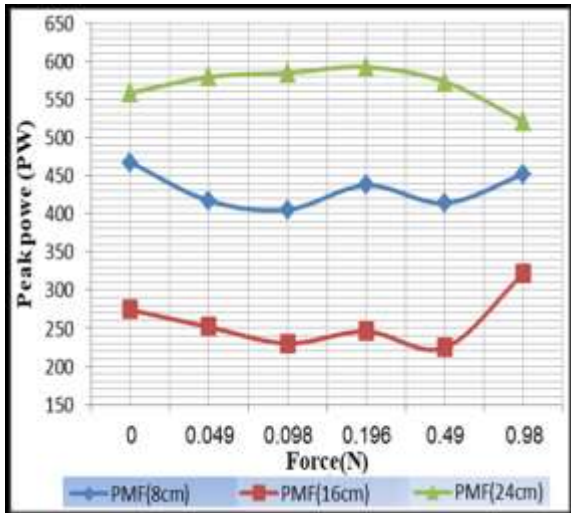
Figure(6): The peak power variation of PM-MZI with (8,16,24cm) and different forces applied on the micro cavities splicing regions.
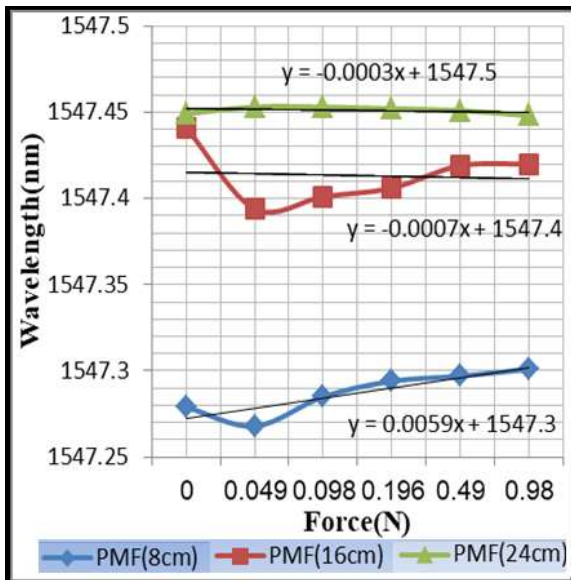
Figure(7): The wavelength variation of PM-MZI with (8,16,24cm) and different forces applied on the micro cavities splicing regions.

4. **Conclusion**

The main points that can be concluded from this work are, the MZI micro-cavities shows high interference and good sensitivity and are thought to be caused by the large force that is applied to a small area. The higher sensitivity 0.00115με obtained after applying 0.098N on the micro-cavity that has higher width and length 24 μm and 12 μm, respectively. When the applied mechanical effect the micro-cavities region, the wavelength shifting is in the blue shift. The results of the interferometer spectral width so widely ring. These results are promising to give

rise to the possibility of getting narrower temporal pulses for communication applications. The highest spectral width 251.58 (μm) has been gaining when the PMF was 16cm in length and0,049 .force applied on micro cavity splicing regions.

References

[1] A.T. Yahiya and T. S. Mansour, "Tunable band pass Filter based on Nested Mach-Zehnder interferometer," J. Eng. Applied Sci.,Vol.13.pp7450-7458,(2018).

[2] Du, H., Sun, X., Hu, Y., Dong, X. and Zhou, J., "High sensitive refractive index sensor based on cladding etched photonic crystal fiber Mach-Zehnder interferometer". Photonic Sensors, 9(2), pp.126-134, (2019).

[3] A. M. Shrivastav, D. S. Gunawardena, Z. Liu and H. Tam, "Microstructured optical fiber based Fabry–Perot interferometer as a humidity sensor utilizing chitosan polymeric matrix for breath monitoring" Scientific Reports, Vol:10, (2020).

[4] S. Deng, H. Meng, X. Wang, X. Fan, Q. Wang, M. Zhou, X. Guo, Z. Wei, F. Wang, C. Tan, and X. Huang, " Graphene oxide-film-coated splitting ratio adjustable Mach-Zehnder interferometer for relative humidity sensing", optics express, Vol. 27, No. 6, (2019).

[5] Q. Wang, W. Wei, M. Guo and Y. Zhao, "Optimization of cascaded fiber tapered Mach–Zehnder interferometer and refractive index sensing technology", Sensors and Actuators B: Chemical, Vol. 222, pp.159-165, (2016).

[6] L. Zhang, S. Sun, M. Li, and N. Zhu, "All-optical temporal fractional order differentiator using an in-fiber ellipsoidal air-microcavity," Journal of Semiconder., Vol. 38, No. 12, pp. 126001, (2017).

[7] F. Q. Mohammed, T,S. Mansour and A. W. Abdul wahhab, " A tunable Mach–Zehnder interferometer based on dual micro‑cavity photonic crystal fiber for load measurement, " Photon Netw Commun. Vol.38,pp. 270-279 (2019).

[8] M. Chena, Y. Zhaoa,_, H. Wei and S.Krishnaswamyc, "Cascaded FPI/LPFG interferometer for high-precision simultaneous measurement of strain and temperature", Elsevier, Vol. 53, No.102025 ,(2019).

[9] X. Dong, H. Du, Z. Luo and J. Duan, "Highly Sensitive Strain Sensor Based on a Novel Mach-Zehnder Interferometer with TCF-PCF Structure" *Sensors*, Vol. 18, No. 1: 278, (2018).

[10] V. L. Kalyani and V. Sharma, "Different types of Optical Filters and their Realistic Application," J. Manag. Eng. Inf. Technol, Vol. 25, No. 33, pp. 2394–8124, (2016).

[11] C. Aichele, J. Kobelke, J. L. Santos, J. Bierlich, M. S. Ferreira, P. Roriz, O. Frazao, K. Wondraczek, and K. Schuster, et al, "Measuring strain at extreme temperatures with a Fabry-Perot optical fiber sensor," International Conference on Optical Fibre Sensors, vol. 9634, pp. 96343P- 96343P-4, (2015).

[12] X. Dong, X. Sun, D. Chu, K. Yin, Z. Luo, C. Zhou, C. Wang, Y. Hu, and J. Duan, "Micro-cavity Mach–Zehnder Interferometer Sensors for Refractive Index Sensing," IEEE Photonics Technology Letters, Vol. 28, No. 20, pp.2285-2288,(2016).

[13] E. Schena, D. Tosi, P. Saccomandi, E. Lewis, and T. Kim, "Fiber optic sensors for temperature monitoring during thermal treatments: an overview", Sensors, vol. 16, no. 7, p. 1144, (2016).

[14] Y. Wang, S. Wang, L. Jiang, H. Huang, L. Zhang, P. Wang, L. Lv, and Z. Cao, "Temperature-insensitive refractive index sensor based on Mach-Zehnder interferometer with two micro cavities," Chin. Opt. Lett., Vol.15, pp.020603, (2017).

[15] R. Zhao, T. Lang, J. Chen and J. Hu, "Polarization-maintaining fiber sensor for simultaneous measurement of the temperature and refractive index ," Optical Engineering, Vol. 56, pp. 057113,(2017).

[16] D. Dobrakowski, A. Rampur, G. Stępniewski, A. Anuszkiewicz, J. Lisowska, D. Pysz, R. Kasztelanic and M. Klimczak, "Development of highly nonlinear polarization maintaining fibers with normal dispersion across entire transmission window ," J. Op, Vol.21, No.1, pp. 015504, (2018).

[17] G. Rajan, K. Iniewski, S.R. Sharma, J. E. Morris, A.Tekin and Ahmed Emira, "Optical Fiber sensors advanced Techniques and Applications", Canada: CRC Press by Taylor & Francis Group,(2015).

[18] F. M. Abdulhussein, M. Hou, S. Liu, T. S. Mansour, and P. Lu, "Integrated Fabry-Perot/Fiber Bragg Grating Sensor for Simultaneous Measurement, " in CLEO: 2015, OSA Technical Digest (online) (Optical Society of America, (2015),

[19] T. S. Mansour and F.M. Abdulhussein, "Dual Measurements of Pressure and Temperature With Fiber Bragg Grating Sensor", Vol.11,pp.86-91,(2015).

[20] S. H. Mahmood ,T.S. Mansour, Y.I. Hammadi and L. Tariq "Pulse compression by using 7 and 19 cells 1550 hollow core photonic crystal fiber", Eng, Applied sci.,Vol.13,No.17,pp.7198-7204,(2018).

[21] F. Q. Mohammed and T.S. Mansour, "Design and Implementation Tunable Band Pass Filter based on PCF-Air Micro-cavity FBG Fabry-Perot Resonator, " Iraqi Journal of Laser, Vol. 18, No. 1, pp. 13-23, (2019).

[22] B. H. Mutar ,N. Faris, Y. I. Hammadi and T. Mansour, "In-Line Fiber Tunable Pulse Compressor using PM-Mach Zehnder Interferometer, " Journal of Mechanical Engineering Research and Developments. Vol. 44 ,pp. 287-297 , (2021).

[23] Y. Wang, S. Wang, L. Jiang, H. Huang, L. Zhang, P. Wang, L. Lv, and Z. Cao, "Temperature-insensitive refractive index sensor based on Mach-Zehnder interferometer with two micro cavities," Chin. Opt. Lett., Vol.15,No.2, pp.020603, (2017).

[24] N. Dash and R. Jha, "Fabrication of Inline Micro Air Cavity With Choice-Based Dimensions, " IEEE Photonics Technology Letters, Vol. 29, No. 14, pp. 1147-1150, (2017).

[25] E. Labasova, "Determination of Modulus of Elasticity and Shear Modulus by the Measurement of Relative Strains ," Research Papers Faculty of Materials Science and Technology Slovak University of Technology, Vol.24, (2016).

[26] T. Vo , B. Reeder , A. Damone and P. Newell, "Effect of Domain Size, Boundary, and Loading Conditions on Mechanical Properties of Amorphous Silica:A Reactive Molecular DynamicsStudy",Nanomaterials,Vol.10,No.54,(2019).

تصميم مرشح تمرير النطاق البصري المستند على المتداخل المتراصف ماخ-زندر باستخدام الالياف المحافظة على الاستقطاب

براء حسن مطر   تحرير صفاء منصور

معهد الليزر للدراسات العليا / جامعة بغداد – بغداد / العراق

الخلاصة: في هذا البحث ، تم تقديم مرشح تمرير النطاق المتباين المستند على مقياس التداخل المتراصف المحافظ على الاستقطاب من نوع ماخ-زند. يتم تنفيذ قابلية ضبط مرشح تمرير النطاق من خلال تطبيق قوى ميكانيكية مختلفة N على مناطق التجاويف الدقيقة (MCSRs). يتكون التجويف الدقيق باستخدام ثلاثة أطوال متغيرة من الألياف أحادية النمط المحافظة على الاستقطاب بطول (24،16،8) سم ، يتم ربطها بين جزأين من (SMF-28) بطول (26،13) سم ، باستخدام تقنية اللحام الكهربائي. تم تحقيق متناهيه في الصغر تجريبيا تجاويف بيضوية الشكل بالتوازي مع محور الانتشار بأبعاد تتراوح بين (12-24) مايكرومتر للعرض و (4-12) مايكرومتر للطول. يكون للتجويف الصغير بعرض وطول يصلان إلى 24 مايكرومتر و 12 مايكرومتر أعلى حساسية تبلغ 0.00115 مايكرومتر عند تطبيق 0.098 نيوتن على التجويف الدقيق. وابضا تم الحصول على FWHM (251.584) بيكو متر عندما كان طول الليف البصري الحفاظ على الاستقطاب 16 سم بعد تطبيق 0.49 نيوتن على منطقة التجويف الدقيق . مصدر الليزر النبضي المستخدم في هذه التجربة له ذروة تبلغ 1.2297 ميغاوات ، FWHM 286 بيكو متر, ويتركز عند الطول الموجي 1546.7 نانومتر.